ORIGINAL PAPER

CrossMark

Use of poly[ionic liquid] as a conductive binder in lithium ion batteries

Susana Chauque[1] · Fabiana Y. Oliva[1] · Osvaldo R. Cámara[1] · Roberto M. Torresi[2]

Abstract
In the present work, we studied the performance of different new binders based on poly[ionic liquids] (POILs) using a well-known negative electrode material such as $Li_4Ti_5O_{12}$ (LTO) compound and ionic liquids (ILs) as solvents. We used an IL formed by $Pip_{1,4}Tf_2N$ with N-butyl-N-methyl piperidinium ($Pip_{1,4}$) as the cation and bis(trifluoromethanesulfonyl)imide (Tf_2N^-) as the anion. We tested two POILs as binders, composed of either $LiTf_2N$, $Pip_{1,4}Tf_2N$, and PVDF or poly[diallyldimethylammonium]Tf_2N (PDDA) as the polymer precursors (PVDF-IL and PDDA-IL, respectively). The best Li^+ transport number as well as the smallest contact angle (electrolyte membrane) was obtained for the PDDA-IL polymer. The swelling effect better facilitates impregnation than the other polymers. The LTO/PDDA-IL combination showed the best specific capacity, 70 mAh g^{-1}, and a stable prolonged cycling. We identified the Ti^{IV}/Ti^{III} redox reversible processes by cyclic voltammetry experiments and the differential capacity profiles. Additionally, we measured the Li^+ diffusion coefficient to be approximately 10^{-12} cm^2 s^{-1}. When different binders and IL-solvents are employed in a typical LTO cell, we demonstrated that the factors that determine cell performance are the ionic conductivity and the swelling effect.

Introduction

The most important challenges nowadays regarding the use of renewable energies consist of achieving proper storage systems, particularly those that can be applied in vehicle transportation in order to replace the conventional use of fossil fuels. These kinds of storage systems should have the highest efficient rechargeable batteries with a safe handling system as well as a long life span and high specific energy storage capacities (in terms of both mass and volume) [1, 2]. The most promising storage technology is the rechargeable lithium ion batteries (LIBs), which are currently used in small electronic devices and can potentially be applied in hybrid and electric vehicles (HVs and EVs, respectively) [3–5]. The main reason is that these types of battery are considered as the most suitable energy storage technology that can be used as a power source for passenger vehicles without adding excessive weight, besides other purposes such as high-performance stationary and delocalized energy systems. Currently, commercial LIBs employ organic liquids with high dielectric constant as solvents (e.g., ethylene carbonate, dimethyl carbonate), which are highly suitable for the dissolution of lithium salts used as electrolyte. These solvents also show a large electrochemical window of stability of approximately 4.5 V, which makes them adequate for high-voltage batteries [6]. Nevertheless, in general, LIBs are operated in voltage regions exceeding the stability window of the organic solvents. Therefore, they have a potential safety risk, especially under overload conditions, which shortens the useful voltage range. On the other hand, the electrolyte breakdown—which is the main critical degradation mechanism in current commercial LIBs—is prevented by the formation of a homogeneous and stable electron-insulating solid electrolyte interphase (SEI) on the particles of active material in the negative electrode during the first charge-discharge cycle. Also, the SEI lets the conduction of lithium ions through its structure in such a way that the overall current flow is enabled. However, there are serious drawbacks of employing these high vapor pressure organic solvents. Overpressures caused by battery short circuit or overheating may result in explosions. These unfortunate accidents have caused the gain of some negative notoriety concerning the use of LIBs among consumers. Thus, the

✉ Roberto M. Torresi
rtorresi@iq.usp.br

[1] Instituto de Investigaciones en Fisicoquímica de Córdoba, Facultad de Ciencias Químicas, Universidad Nacional de Córdoba, Av. Medina Allende y Haya de la Torre, Córdoba, Argentina

[2] Departamento de Química Fundamental, Instituto de Química, Universidade de São Paulo, Av. Prof. Lineu Prestes, 748, São Paulo, Brazil

Springer

research focused on the replacement of organic solvents has received attention due to its capability to increase safety and stability of LIBs [4, 7]. Ionic liquids (ILs) as potential electrolytes have gained considerable interest due to their thermal and electrochemical stabilities, flame retardant performance, and negligible vapor pressure [8]. Among other typical cations of ILs, N-butyl-N-methyl piperidinium ($Pip_{1,4}$) is one of the most common, and it is employed by many research groups in different areas, especially in energy storage devices. On the other hand, the anion bis(trifluoromethanesulfonyl)imide, $[(CF_3SO_2)_2N^-]$ or (Tf_2N^-), has been broadly investigated too, since the ILs formed by this anion have low viscosity, high ionic conductivity, and hydrophobic properties [9].

Otherwise, the safety of the negative electrode materials is an ongoing research subject since graphite has a fragile structure, decreasing the prolonged lifetime in charge/discharge cycling. Therefore, the search of new materials to build better and safer anodes is a technological requirement [10]. Additionally, the composition and structure of the SEIs formed on graphite have already been studied extensively [11, 12]. Lithium titanate ($Li_4Ti_5O_{12}$ or LTO) can be potentially one of the best candidates as an active material for the negative electrode of safer LIBs, even better than graphite, due to several reasons such as the following: the lithium insertion process occurs at a higher potential than the lithium metal deposition, and LTO is a "zero-strain" material with only a slight change in unit cell volume when lithium ions are intercalated or deintercalated, resulting in a high lifetime for charge/discharge cycling [2, 13–18]. However, LTO-negative electrodes still show severe gas release processes when they are put in contact with the conventionally used organic electrolytes (alkyl carbonates). Thus, it results in battery swelling and drawbacks related to film formation on the anode surface [19]. It was proposed that stable SEI layers are effective, suppressing further electrolyte decomposition and reducing the gassing effect of LTO-based batteries [19].

The main goal of this work is to employ a well-known negative active material such as LTO in order to characterize different binders using ionic liquids as solvent. Particularly, we investigate the electrochemical behaviour of pristine LTO as negative electrode with an electrolyte formed by $Pip_{1,4}$ as the cation, and Tf_2N^- as the anion, and lithium bis(trifluoromethanesulfonyl)imide ($LiTf_2N$) as the lithium salt. The LTO used was synthesized by the ceramic method and without any subsequent post treatment. The electrochemical response of LTO-specific charge capacity and the lithium ion intercalation/de-intercalation behaviour in this kind of system depend on the binder employed. Therefore, two different poly[ionic liquid] (POIL) were synthesized to be used as a binder with the following composition: a polymer precursor, $LiTf_2N$ and $Pip_{1,4}Tf_2N$ [20–22]. The precursors employed to synthesize both POILs were polyvinylidene fluoride (PVDF) and poly [diallyldimethylammonium]Tf_2N (PDDA) [23].

Additionally, for comparison, commercial PVDF was employed as a typical binder of negative electrodes. To characterize the prepared polymers and to evaluate their properties (to be used as binders in the negative electrodes of LIBs), parameters such as ionic conductivity, Li^+ ion transport number, and contact angle were measured on membranes prepared with the different polymers that have been used. The LTO-negative electrodes prepared using the characterized binders were tested in Swagelok® T-cells (LTO-lithium metal cells). Cyclic voltammetry and galvanostatic charge-discharge experiments were performed to characterize the lithium ion intercalation/de-intercalation response, to evaluate the specific charge storage capacity and the cycling performance, and to obtain the diffusion coefficient of the Li^+ ion in the host matrix of LTO in the IL electrolytes.

Materials and methods

Materials Polyvinylidene fluoride (PVDF), N-butyl-N-methyl piperidinium bis(trifluoromethanesulfonyl)imide ($Pip_{1,4}Tf_2N$), lithium bis(trifluoromethanesulfonyl) imide ($LiTf_2N$), and poly[diallyldimethylammonium]chloride (PDDA: 20% w/w solution in water and MW = 100,000–200,000).

LTO and IL preparation $Li_4Ti_5O_{12}$ was prepared by a solid-state method, as described in Chauque et al. [24]. The IL employed was prepared as described by Bazito et al. [25].

Polymer membrane preparation Three different kinds of membranes were prepared in order to study the physicochemical properties of each polymer to be used as a binder in the preparation of the LTO-negative electrodes of the LIBs. A membrane of PVDF was prepared by dissolving 1 g of the polymer in 10 mL of N-methyl-2-pyrrolidone (NMP) as the solvent. In addition, as proposed by Benedetti and Torresi [21], two types of POILs were prepared by adding IL and $LiTf_2N$ as lithium salt, which in all cases had the following composition: $50_{Polymer}:50_{IL}$ with the incorporation of 4.8% of lithium salt to obtain 1 g of each POIL (using PVDF and PDDA as the polymers) in 10 mL of an adequate solvent (NMP for PVDF and acetone for the PDDA polymer). The three prepared polymer solutions were placed over glass substrates to form the polymer membranes. Then, the solvent was left to evaporate at room temperature, avoiding the formation of air vesicles in the resulting membrane, prior to a drying process under vacuum at 60 °C for 12 h. The polymer membranes obtained were named as follows: PVDF, PVDF-IL, and PDDA-IL, according the polymeric precursor employed. Prior to use, all the materials prepared (ILs and membranes) were maintained under an argon atmosphere in a glovebox (LabMaster 130) with H_2O and O_2 contents < 0.1 ppm.

Table 1 shows a summary of all the prepared membranes and corresponding employed solvents.

Polymer membrane characterization The experiments measuring ionic conductivity and the Li^+ transport number were performed on disks of each type of membrane using a Swagelok® cell, assembled in a glovebox with an argon atmosphere. The ionic conductivity of each membrane was determined by electrochemical impedance spectroscopy (EIS), placing the membrane disk between two parallel stainless-steel electrodes in the frequency range of 10 Hz to 100 kHz. The Li^+ transport number t_{Li^+} through each membrane was determined from EIS and chronopotentiometry measurements using a membrane thickness of 150 μm placed between two thin disks of metallic lithium. Contact angle experiments on each membrane were performed under an air atmosphere using a Digidrop MCAT-GBX Instrumentation Scientifique instrument coupled to a Nikon Pixelink camera. The measurements were performed by slowly placing a drop of 2.0 μL of the electrolyte used on the electrochemical measurement (1.0 mol L^{-1} of the lithium salt $LiTf_2N$ in the ionic liquid $Pip_{1,4}Tf_2N$ as the solvent) on the prepared membrane and then measuring the angle formed between the electrolyte-membrane contact and the air-electrolyte tangent line at the insertion point.

Electrochemical characterization of each LTO/binder combination To characterize the lithium ion charge/discharge response, cyclic voltammetry and galvanostatic charge/discharge experiments were performed using the three-electrode Swagelok®-type cell (T cell) assembled in a glovebox chamber. The working electrode was prepared using a mixture of synthesized active material (LTO) and carbon black (Timcal Super P, added to increase the electrical conductivity), and each polymer described before (PVDF and the two POILs, PVDF-IL and PDDA-IL) was employed as a binder at a weight ratio of 80:10:10, respectively. The mixture was dispersed in NMP (with PVDF and PVDF-IL binders) or acetone (with a PDDA-IL binder) as solvent and agitated for 12 h to ensure homogeneous dispersion. The slurry obtained was coated onto copper foils (15 μm in thickness), dried in an oven at 80 °C for 12 h, and pressed by applying 10 t cm^{-2}. The

coated foils were punched into 8-mm-diameter disks to obtain the working electrode and were maintained in a glovebox before cell assembly. The obtained electrodes were named as follows: LTO/PVDF, LTO/PVDF-IL, and LTO/PDDA-IL according the binder employed (PVDF, PVDF-IL, and PDDA-IL, respectively). The total mass deposited on each electrode was approximately 1 mg cm^{-2}. Two lithium metallic disks (10 mm in diameter) were used as the reference and counter electrodes with Celgard® membrane disks as spacers between the three electrodes. All the potential values reported hereafter are referred to as the Li^+/Li^0 couple standard potential. Finally, the electrolyte employed was a solution prepared by dissolving 1.0 mol L^{-1} of the lithium salt $LiTf_2N$ in the ionic liquid $Pip_{1,4}Tf_2N$ as the solvent. After the cell assembly, it was allowed to reach equilibrium following open circuit potential (OCP)-time to be sure that the electrolyte fully fills the electrode pores avoiding viscosity issues. Cyclic voltammograms (CVs) were performed at a 1.0 mV s^{-1} scan rate in the potential range from 3.0 to 0.6 V in order to determine the Ti(IV)/Ti(III) redox couple peak potentials and the electrochemical stability. For each LTO-lithium cell, ten galvanostatic charge/discharge (GCD) cycles were performed within the interval from 3.0 to 0.6 V at a current value of 0.5 C to analyse the specific capacity of the different cells using each binder synthesized and expressed as mAhg^{-1} (in terms of the mass of the active material, LTO). To obtain the diffusion coefficient from the *Sand* equation, additional GCD cycles were performed at successively higher applied current values of charge and discharge (0.5, 1, 2, 3, 4, 5, and 10 C) in the same voltage range. All the electrochemical experiments were performed with an Autolab PGSTAT30 (Metrohm) potentiostat/galvanostat controlled by the software NOVA1.10.

Results and discussion

Characterization of the binder membranes All the membranes synthesized showed good compatibility between the components since no phase separation or IL segregation was observed. In addition, the membranes prepared with an IL in their structure presented more flexibility and transparency. To calculate the ionic conductivity of each membrane prepared, classic AC impedance experiments were performed to obtain the respective resistances. The ionic conductivity (σ) was calculated by the following equation [26]:

$$\sigma = \frac{l}{A\,R} \tag{1}$$

where l is the membrane thickness (150 μm), A is the electrode area (0.5 cm^2), and R is the membrane resistance obtained from EIS experiments by an extrapolation of the real part of the impedance at high frequencies. In the PVDF-based

**Table 1** Compositions of the different prepared polymer membranes and the corresponding employed solvents

Polymer membrane	Solvent	Mass/g		
		Polymer	IL	LiTf$_2$N
PVDF	NMP	1.0	0.0	0.0
PVDF-IL	NMP	1.0	1.0	0.1
PDDA-IL	Acetone	1.0	1.0	0.1

membranes, it was observed that the addition of the IL and lithium salt increases the ionic conductivity by one order of magnitude. Of all the studied membranes, the PDDA-IL showed the highest ionic conductivity, in agreement with the results obtained by Benedetti and Torresi [21]. Due to the feasibility of the application of the studied polymers as new lithium ion binders, the Li$^+$ transport through these binder membranes is a relevant parameter to be analysed. The transport number of Li$^+$ t_{Li^+} was obtained using a technique proposed by Evans et al. [27] and is used by many authors for polymeric electrolytes [28, 29]. This technique consists of the following: an EIS determination at an open circuit potential and a dc polarization followed by a second EIS measurement at the polarization potential. All the experiments were performed on a symmetrical cell with each membrane placed between two thin disks of lithium metal as the electrodes. t_{Li^+} was calculated by Eq. 2:

$$t_{Li^+} = \frac{I_s(\Delta V - I_0 R_0)}{I_0(\Delta V - I_s R_s)} \tag{2}$$

where t_{Li^+} is the Li$^+$ transport number; ΔV is the applied polarization potential of 10 mV; I_0 and I_s are the initial and steady state current values, respectively; and R_0 and R_s are the initial and steady state measured resistances, respectively. Figure 1 shows EIS and chronoamperometry measurements as an example to calculate t_{Li^+} and then confirm the viability of PVDF-IL and POIL to be used as the binders for negative electrode preparation. Figure 1a shows a plot of the current as a function of time at $\Delta V = 10$ mV, and in Fig. 1b, the Nyquist diagrams at the OCP and applied $\Delta V = 10$ mV are represented. From the Nyquist diagrams, R_0 and R_s were obtained for each membrane prepared. The results show that, at the same lithium salt concentration in both membranes, t_{Li^+} increases from 0.05 (with PVDF as the polymer precursor) to 0.20 (with PDDA as the precursor). The value of 0.20 obtained for the PDDA-IL is remarkable, considering that the lithium ion concentration is in ionic media. In addition, similar values of t_{Li^+} were reported in other systems based on POILs [30].

To analyse the interaction and chemical affinity between the binder membrane and the electrolyte, contact angle determination is an important macroscopic factor to consider. This parameter is crucial since it is important to ensure the complete penetration of the electrolyte into the pores of the active material film, which allows the Li$^+$ ions to have full access to the surface of the LTO particles. The results obtained from the contact angle measurements show that for all the binder membranes, the angle formed between the air-electrolyte and electrolyte-membrane lines were below 90°, i.e., 45° for PVDF, 36° for PVDF-IL, and 32° for PDDA-IL. These results indicate that all the prepared membranes have the ability to be wetted by the electrolyte. The PDDA-IL membrane shows the lowest electrolyte-surface contact angle, resulting in excellent
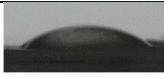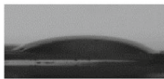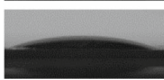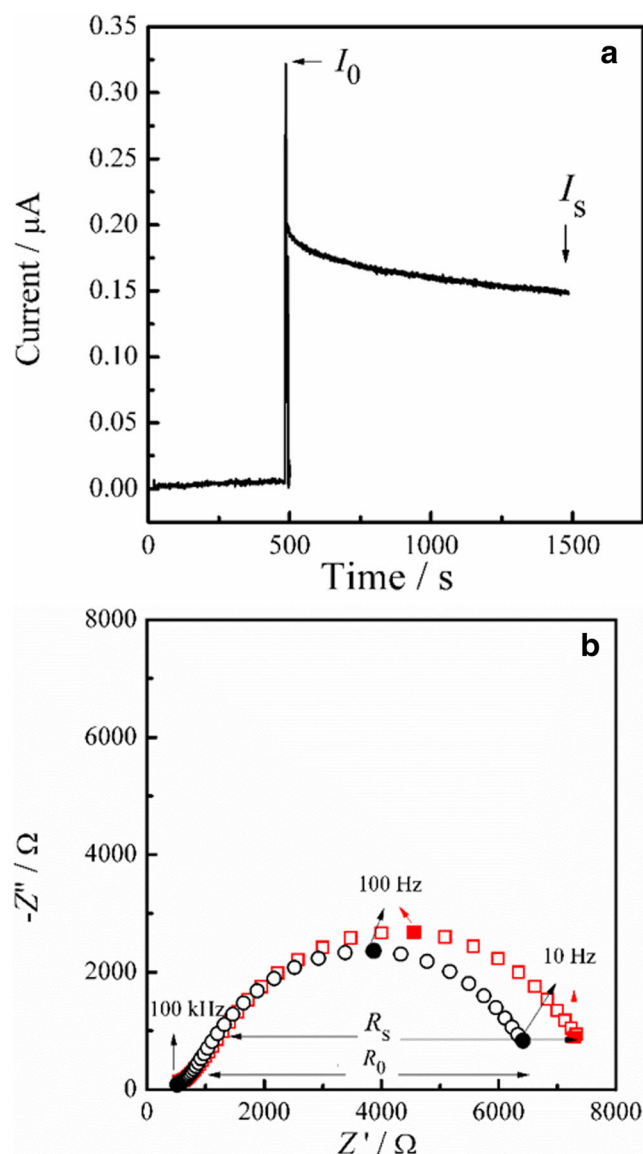

Fig. 1 Experiments for determination of the Li$^+$ transport number in the PDDA-IL membrane. **a** Current as a function of time at an applied potential (ΔV) of 10 mV. **b** Nyquist diagrams from 100 kHz to 10 Hz at OCP (black) and an applied potential of 10 mV (red)

wetting properties. This property allows us to propose that the PDDA-IL compound is most suitable as an appropriate binder in the active material film preparation for the LTO-based negative electrode. The results in terms of the physicochemical properties of ionic conductivity, Li$^+$ transport number, and contact angle are summarized in Table 2.

Due to the increase in the affinity between the electrolyte and membranes (in the following order: PVDF, PVDF-IL, and PDDA-IL), it is possible to establish the existence of a tendency in membrane swelling in the presence of the IL electrolytes. From this trend, the behaviour of POILs when used as binders on the negative electrodes for IL-based LIBs can be predicted. The IL-swelling effect (or impregnation) is not as efficient as in the case of organic solvents (and PVDF as a binder).

Table 2 Ionic conductivity, Li$^+$ transport number, and contact angle measured for each polymer membrane

Polymer membrane	Ionic conductivity/µS cm^{-1}	t_{Li^+}	Contact angle	
PVDF	0.25	--		45°
PVDF-IL	3.88	0.05		36°
PDDA-IL	47.8	0.20		32°

**Electrochemical characterization of each LTO/binder combination** Figure 2a shows the CV profiles performed at 1.0 mV s^{-1} in the potential range of 3.0 to 0.6 V for all the LTO/binder combinations studied in this work employing Pip$_{1,4}$Tf$_2$N as the solvent. Nevertheless, the CV profile for LTO/PVDF was performed from 3.0 to 1.0 V in order to maintain the same experimental conditions used in our previous work using a typical mixture of organic solvents (ethylene carbonate (EC) and dimethyl carbonate (DMC) solvent mixture, 1:1 by mass) containing 1.0 mol L^{-1} LiPF6 salt as the electrolyte [24]. When PVDF is used as the binder, the peak potential corresponding to the reduction of Ti(IV) to Ti(III), which should appear at 1.55 V when organic solvents are employed [24], is absent, showing that lithium ion insertion into the host matrix of LTO (which requires the Ti(IV)/Ti(III) reduction process) does not occur. When the binder employed is changed to either kind of POIL, it can be observed that the peak potential of the reduction process occurs at shifted potentials, i.e., approximately 1.4 V for LTO/PVDF-IL and 1.3 V for LTO/PDDA-IL systems. The CV profile corresponding to the LTO/PDDA-IL combination shows the highest current density values; however, the more reversible response is observed for the LTO/PVDF-IL combination with a well-defined redox Ti(IV)/Ti(III) peak and a lower ΔE_{peak}. In addition, the charge density involved in each CV curve (Fig. 2b) increases in the following sequence: PVDF, PVDF-IL, and PDDA-IL, which is in agreement with the increase in the ionic conductivity of the binder employed, as shown in Table 2. By comparing LTO/PVDF with LTO/PVDF-IL, it is possible to observe that the addition of IL and lithium salt in the binder composition improves the lithium-ion insertion process, and this result can be related to the observed enhancement in the ionic conductivity of the binder polymer.

To study the electrochemical performance in terms of the storage capacity for the combinations of LTO/binder with the ion insertion/de-insertion processes observed in the CV experiments, GCD curves were obtained at constant current densities of 20 and 26 mA g^{-1} for LTO/PVDF-IL and LTO/PDDA, respectively, in the voltage interval from 3.0 to 0.6 V. The charge/discharge curves corresponding to the 10th cycle for all electrodes studied are shown in Fig. 3a, where the reported specific capacities refer to the LTO mass in the electrode coating. In both cases, an almost flat plateau can be observed at approximately 1.55 V, which is characteristic of the two-phase reaction based on the Ti(IV)/Ti(III) redox inner couple [24]. The cycling performance (specific capacity of charge and discharge) and the Coulombic efficiency for both electrodes revealed a great stability of the active materials during the first 10 cycles, as displayed in Fig. 3b. Note that the highest specific capacity and the most reversible charge/discharge performance were obtained from the LTO/PDDA-IL combination (70 mAh g^{-1}) compared to the LTO/PVDF-IL electrode (54 mAh g^{-1}). Nevertheless, the electrochemical behaviour
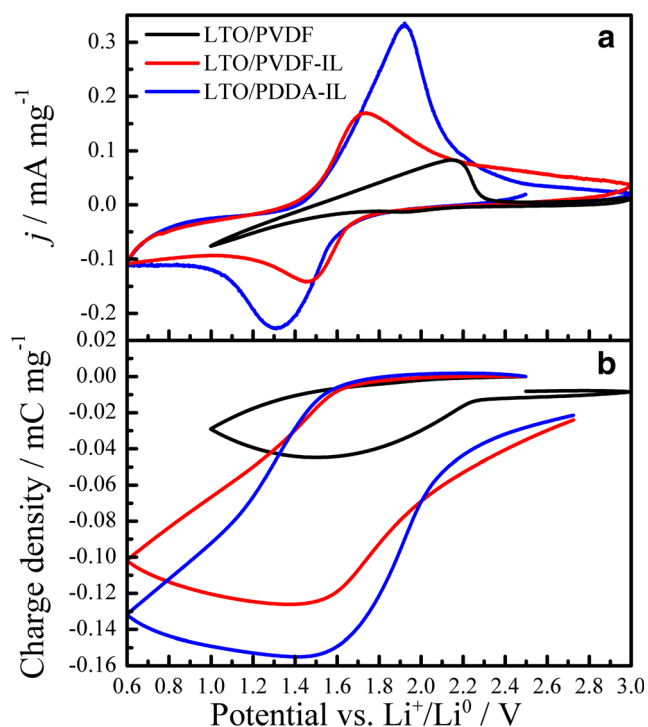
Fig. 2 **a** CV profiles at 1.0 mV s^{-1} for all combinations of LTO/binder in 1.0 mol L^{-1} LiTf$_2$N using Pip$_{1,4}$Tf$_2$N as solvent. **b** Charge density of the CVs shown in (**a**) versus potential
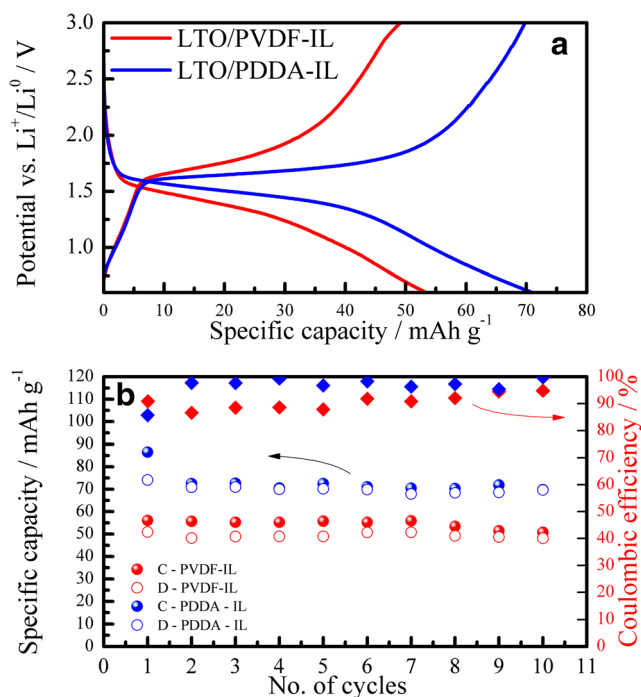
Fig. 3 **a** GCD profiles corresponding to the tenth cycle for LTO/PVDF-IL (red) and LTO/PDDA-IL (blue) in 1.0 mol L^{-1} LiTf$_2$N using Pip$_{1,4}$Tf$_2$N as the solvent. **b** Charge/discharge performance and the Coulombic efficiency calculated for each negative electrode

obtained using organic solvents and PVDF as the binder was different, in which the measured specific capacity of LTO was approximately 110 mAh g^{-1} and the GCD profiles show a flat

plateau during the whole process [24]. On the other hand, we find that when the organic solvents are replaced by ILs in the LIB systems, the employed binder and its ionic conductivity as well as the swelling effect become crucial factors to consider in the negative electrode design.

Moreover, it is possible to obtain another information from the derivative curves of the GCD cycles. An important indicator of the degradation and occurrence of an electrochemical process in a cell is the differential capacity (Q_{diff}) and is given by

$$Q_{diff} = \frac{dq}{dV} \tag{3}$$

where dq/dV is the derivative of the amount of charge added in the charge cycle or removed during the discharge cycle with respect to the cell voltage. When the differential capacity is plotted as a function of the cell voltage, the peaks of the resulting curves can be related to the redox process involved and consequently its respective lithium insertion/de-insertion in the host matrix of the negative electrode material [31]. Figure 4a shows the Q_{diff} curves obtained from the differential capacity of the GCD curves for each LTO/binder combination (from the tenth cycle shown in Fig. 3a). These curves are compared with the respective CV plots in Fig. 4b. Good correlation was observed between both results, where the potential peaks are in accordance with the redox Ti(IV)/Ti(III) couple observed during the CV experiments. Therefore, from these results, it can be confirmed that the

Fig. 4 **a** Differential capacity (Q_{diff}) as a function of cell voltage curves at the 1st cycle (continuous line) and the 10th cycle (dash line). **b** CV profiles at 1.0 mV s^{-1} for LTO/PVDF-IL (red) and LTO/PDDA-IL (blue) in LiTf$_2$N 1.0 mol L^{-1} using Pip$_{1,4}$Tf$_2$N as the solvent
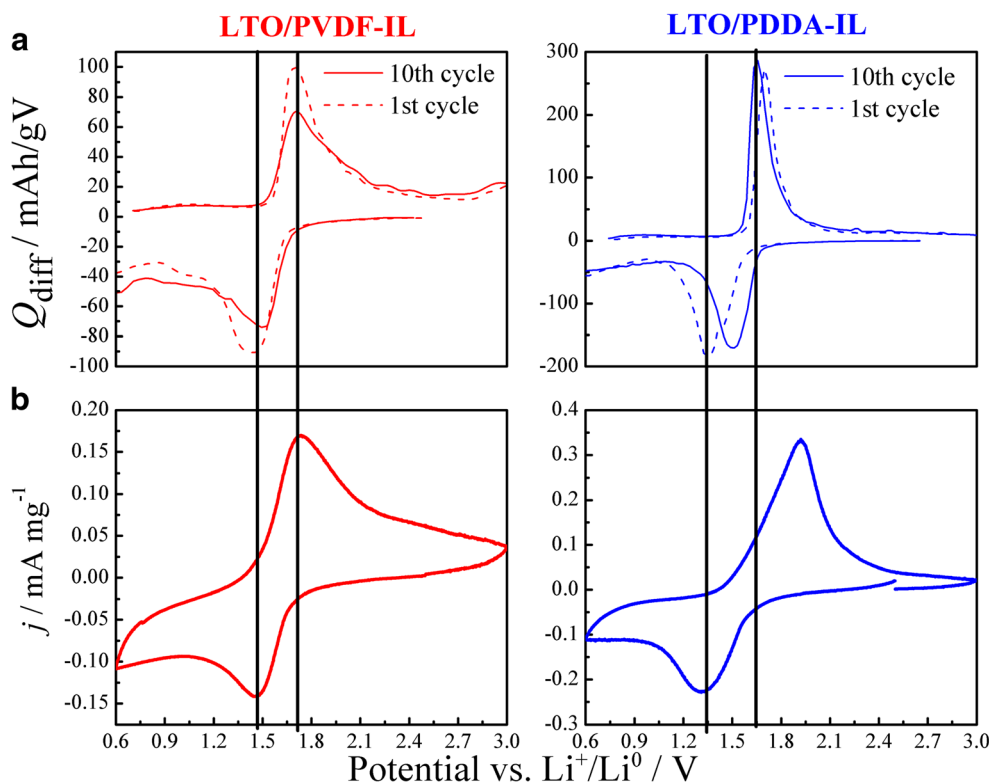
redox processes occur reversibly, and consequently, the insertion/de-insertion processes of lithium ions are carried out. In Fig. 4a, the differential capacity curve corresponding to the first (dashed line) charge-discharge cycle was also included for both LTO/binder combinations in order to analyse the behaviour through the cycling process. For the LTO/PVDF-IL electrode, the peak positions are maintained almost unvaried along the life cycles, which is the ideal behaviour [32]. However, a decrease in the charge involved is also observed by comparing the first and tenth cycles, which is associated with a loss in the storage capacity. For the LTO/PDDA-IL electrode, the results show an improvement in the reversibility of the lithium ion insertion/de-insertion processes with life cycle. Additionally, the charge remains constant, which represents an important improvement with respect to the other electrode.

Finally, to determine the diffusion coefficient of lithium ions in the host matrix of LTO, GCD measurements were performed at different current values. The diffusion coefficients were obtained from the *Sand* equation [26] (Eq. 4), which relates the constant applied current (i) in a galvanostatic pulse with the transition time τ (here considered the length of time at the plateau potential).

$$\frac{i\tau^{1/2}}{Co^*} = \frac{n\,F\,A\,Do^{1/2}\pi^{1/2}}{2} \tag{4}$$

Here, C_o^* is the concentration of lithium ions in moles per cubic centimetre, n is the number of electrons transferred, F is the Faraday constant, A is the geometric electrode area, and D_o is the diffusion coefficient. From each GCD curve, the durations of the charging and discharging plateau (τ) were obtained, and the diffusion coefficient values were calculated for the charge (cathodic diffusion coefficient) and discharge (anodic diffusion coefficient) processes. Figure 5 shows the linear dependence of $\tau^{1/2}$
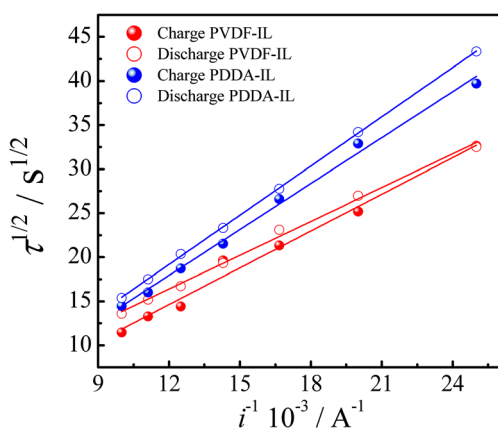
Fig. 5 Dependence of the square root of transition time ($\tau^{1/2}$) for charge and discharge potential plateaus as a function of the inverse of the applied current (i^{-1})

versus i^{-1} for both LTO/binder combinations that showed adequate lithium ion insertion/de-insertion behaviour.

The obtained diffusion coefficient values for the two analysed LTO/binder combinations were almost identical, resulting in an average value of $(1.5 \pm 0.5)\,10^{-12}$ cm^2 s^{-1}. It is interesting to highlight that these values are similar to the diffusion coefficients of lithium ions obtained from CV experiments at different scan rates using EC/DMC organic solvents and LiPF$_6$ as the electrolyte [24]. All these coefficient values are characteristic of an ion diffusion process into a solid matrix.

The ionic conductivity, lithium ion transport number, and IL swelling effect are different properties directly related to the applicability of these polymers as binders in the preparation of active material slurries for IL-based LIBs. In addition, it can be ensured that the behaviour of LTO as the negative electrode in IL systems depends strongly on the binder employed. In general, when any type of POIL is employed during electrode preparation, the lithium ion insertion/de-insertion processes in an IL system occur more reversibly, and the charge involved is greater than that for the PVDF binder tested under the same experimental conditions. This behaviour can be explained by the fact that the POIL has a higher ionic conductivity and is also prepared with 5% lithium salt (LiTf$_2$N), presenting the ability to be swollen by the IL and allowing the entrance of lithium ions into the solid LTO matrix. The best electrochemical response was obtained when PDDA-IL was used as the negative electrode binder. The PDDA-IL-based binder exhibited a better interaction with the IL solvent; therefore, it allowed favourable lithium ion conduction into the deposited film containing the LTO active material.

Conclusions

In the present work, different electrochemical techniques were applied to study two new binders based on poly[ionic liquids] (POILs) and a well-known negative electrode as lithium titanate (LTO) in LIBs using ionic liquids (ILs) as the electrolyte solvent. The results demonstrated that the lithium ion insertion/de-insertion processes in such non-conventional organic solvent media depend strongly on the nature of the binder employed in the electrode design. When a typical PVDF binder is used, lithium ion insertion does not occur; therefore, the LTO material is not able to store electric charge. Thus, two types of POILs were prepared using PVDF and PDDA as polymer precursors. The addition of IL and lithium salt to improve the chemical compatibility with the IL media was evaluated as possible binders. To characterize some physicochemical properties of these polymers, the materials were prepared as membrane-type substrates, and the ionic conductivity, Li$^+$ transport number, and electrolyte-IL contact angle were obtained. If all the membranes are compared, then the ionic conductivities increase in the sequence PVDF < PVDF-

IL < PDDA-IL. The highest Li$^+$ transport number as well as the lowest contact angle value between the electrolyte and the membrane was obtained for the PDDA-IL membrane. This parameter is an important factor to consider since the impregnation of the electrolyte (by the swelling effect) is better than the impregnation of the other membranes. In addition, the electrochemical response of LTO prepared with the PDDA-IL binder (LTO/PDDA-IL negative electrode) was the best observed due to the better charge/discharge-specific capacity and cycling performance. The Ti(IV)/Ti(III) redox reversible processes were identified from CV experiments and were observed from differential capacity (Q_{diff}) vs potential curves obtained for each LTO/POIL tested. On the other hand, the diffusion coefficients obtained for both LTO/POIL systems (LTO/PVDF-IL and LTO/PDDA-IL) were of the same order of magnitude (approximately 10^{-12} cm^2 s^{-1}), which is characteristic of the diffusion process into an LTO solid matrix. To summarize, when LTO is employed as the negative electrode and ILs are used as the electrolyte solvents, the binder nature is crucial. The best LTO electrochemical response, the highest ionic conductivity and Li$^+$ transport number, and the smallest contact angle were obtained using PDDA-IL as a binder.

References

1. Wolfart F, Hryniewicz BM, Góes MS, Corrêa CM, Torresi RM, Minadeo MAOS, Córdoba de Torresi SI, Oliveira RD, Marchesi LF, Vidotti M (2017) J Solid State Electrochem 21(9):2489–2515
2. Armand M, Tarascon JM (2008) Nature 451(7179):652–657
3. Sun X, Radovanovic PV, Cui B (2015) New J. Chem 39:38–63
4. Balducci A (2017) Top Curr Chem 375:1–27
5. Nitta N, Wu F, Lee JT, Yushin G (2015) Mater Today 18(5): 252–264
6. Etacheri V, Marom R, Elazari R, Salitra G, Aurbach D (2011) Energy Environ Sci 4:3243–3262
7. Scrosati JHB, Abraham KM, Schalkwijk W (eds) (2013) Lithium batteries, 1st edn. Wiley, New Jereasy
8. Appetecchi GB, Scaccia S, Tizzani C, Alessandrini F, Passerini S (2006) J Electrochem Soc 153(9):A1685–A1691
9. Martins VL, Sanchez-Ramirez N, Ribeiro MCC, Torresi RM (2015) Phys Chem Chem Phys 17(35):23041–23051
10. Robledo CB, Thomas JE, Luque G, Leiva EPM, Cámara O, Barraco D, Visintin A (2014) Electrochim Acta 140:160–167
11. Peled E, Tow DB, Merson A, Gladkich A, Burstein L, Golodnitsky D (2001) J Power Sources 98:52–57
12. Zhuang GV, Xu K, Jow TR, Ross PN Jr (2004) Electrochem Solid-State Lett 7(8):A224–A227
13. Yuan T, Tan Z, Ma C, Yang J, Ma ZF, Zheng S (2017) Adv Energy Mater 7(12):1601625–1601650
14. Odziomek M, Chaput F, Rutkowska A, Świerczek K, Olszewska D, Sitarz M, Lerouge F, Parola S (2017) Hierarchically structured lithium titanate for ultrafast charging in long-life high capacity batteries. Nat Commun. https://doi.org/10.1038/ncomms15636
15. Sun X, Hegde M, Zhang Y, He M, Gu L, Wang Y, Shu J (2014) Int J Electrochem Sci 9:1583–1596
16. Sun L, Wang J, Jiang K, Fan S (2014) J Power Sources 248:265–272
17. Singh DP, Mulder FM, Wagemaker M (2013) Electrochem Commun 35:124–127
18. Sandhya CP, John B, Gouri C (2013) J Mater Sci 48(17):5827–5832
19. He YB, Li B, Liu M, Zhang C, Lv W, Yang C, Li J, Du H, Zhang B, Kim JK, Kang F (2012) Sci Rep 2(1):913–922
20. Pont AL, Marcilla R, De Meatza I, Grande H, Mecerreyes D (2009) J Power Sources 188(2):558–563
21. Benedetti TM, Torresi RM (2013) Langmuir 29(50):15589–15595
22. Martins VL, Rennie AJR, Lesowiec J, Torresi RM, Hall PJ (2017) J Electrochem Soc 164(13):A3253–A3258
23. Pappenfus TM, Henderson WA, Owens BB, Mann KR, Smyrl WH (2004) J Electrochem Soc 151:209–215
24. Chauque S, Oliva FY, Visintin A, Barraco D, Leiva EPM, Cámara OR (2017) J Electroanal Chem 799:142–155
25. Bazito FFC, Kawano Y, Torresi RM (2007) Electrochim Acta 52(23):6427–6437
26. Bard AJ, Faulkner LR, Swain E, Robey C (eds) (2001) Electrochemical methods: fundamentals and applications, 2nd edn. Wiley, New York
27. Bruce PG, Evans J, Vincent CA (1988) Solid State Ionics 30: 918–922
28. Fernicola A, Croce F, Scrosati B, Watanabe T, Ohno H (2007) J Power Sources 174(1):342–348
29. Yoon H, Howlett PC, Best AS, Forsyth M, Macfarlane DR (2013) J Electrochem Soc 160:1629–1637
30. Ogihara W, Washiro S, Nakajima H, Ohno H (2006) Electrochim Acta 51(13):2614–2619
31. Thompson H (1979) J Electrochem Soc 126(4):608–616
32. Chauque S, Robledo CB, Leiva EPM, Oliva FY, Camara OR (2014) ECS Trans 63(1):113–128